



Unified drift velocity closure relationship for large bubbles rising in stagnant viscous fluids in pipes

Jose Moreiras¹, Eduardo Pereyra*, Cem Sarica², Carlos F. Torres³

McDougall School of Petroleum Engineering, The University of Tulsa, Tulsa, OK 74104, United States

ARTICLE INFO

Article history:

Received 6 November 2013

Accepted 3 September 2014

Available online 16 September 2014

Keywords:

drift velocity

translational velocity

closure relationship

two-phase

slug flow

ABSTRACT

This study investigates the effects of oil viscosity, pipe diameter, and pipe inclination angle on drift velocity. Experiments were conducted for medium viscosity oils using a 0.0508-m ID pipe for inclination angles between 0° and 90°. In these experiments, it was observed that as the liquid viscosity increased, the drift velocity decreased. Drift velocity displayed a convex parabolic behavior with respect to the inclination angle. For all liquid viscosities, a maximum velocity value was observed between 30° and 50° inclinations from horizontal. A unified dimensionless closure relationship for drift velocity is proposed. It was developed using data acquired in this study and available data from literature with a pipe diameter range of 0.0373–0.178 m.

© 2014 Elsevier B.V. All rights reserved.

1. Introduction

Lately, the oil and gas industry turned its focus toward the production of heavier oil, due to the increase and improvement in exploration and drilling technologies, as well as a higher price per barrel of oil and depletion of light oil reserves. In the past, heavy oil reserves were neglected due to the high cost associated with their production, and the lack of proper technology. High density and high viscosity hydrocarbons currently constitute nearly 70% of the available reserves in the world, increasing the need to gain and improve the knowledge of the flow behavior of these fluids.

Most of the multiphase flow models were developed for low viscosity oils. Therefore, these models do not properly consider the effects of viscosity on the flow characteristics and behavior of multiphase flow. Consequently, more comprehensive research to understand the effects of viscosity on multiphase flow is required in order to develop a model that considers liquid viscosity effects.

Gokcal (2005) experimentally studied the effects of high viscosity oil–gas flow. He observed a marked difference between the experimental results for low and high viscosity oils. Additionally, a considerable discrepancy between experimental data and model predictions was reported. Intermittent slug and elongated bubble flow were observed to be the dominant flow pattern. Later,

Gokcal et al. (2008) conducted experiments and developed correlations for slug flow characteristics, taking into account the effects of viscosity. The considered parameters correspond to pressure gradient, drift velocity, transitional velocity, and slug length and frequency. All tests were conducted for horizontal flow and oil viscosities range from 0.121 Pa s to 1.0 Pa s. Kora (2010) conducted experiments and developed correlations for slug liquid holdup in horizontal high viscosity oil–gas flow. Jeyachandra (2011) studied the effect of the inclination angle for horizontal and near-horizontal flow.

In general, all the previous studies in high viscosity oils (0.121 Pa s < μ_o < 1.0 Pa s) demonstrated large differences in two-phase flow behavior as compared to low viscosity oils. In order to clarify the transition between low and high viscosity two-phase flow of hydrocarbons, Brito (2012) conducted an experimental study to analyze the medium viscosity oil (0.39 Pa s < μ_o < 0.166 Pa s) effect on two-phase flow behavior. She analyzed the change in pressure drop, flow pattern, liquid holdup and flow characteristics in a 0.0508-m ID horizontal pipe.

This study aims to understand the medium oil viscosity effect on the drift velocity for medium oil viscosities (0.039 Pa s < μ_o < 0.166 Pa s) in horizontal and upward inclined pipes. Gokcal et al. (2008) conducted drift velocity experiments for high viscosity oils in 0.0508-in. ID pipes and observed that viscosity has a major impact on drift velocity. Later, Jeyachandra (2011) carried out an experimental program considering the same viscosity range as Gokcal et al. (2008) in 0.0762-m and 0.1524-m ID pipes. The previous studies are further expanded to include medium oil viscosities and propose a new drift model. The new closure relationship is valid for a broad range of viscosities, inclination angles (0°–90° from horizontal), and pipe diameters.

* Corresponding author. Tel.: +1 918 6315114.

E-mail addresses: jose-moreirasreynaga@utulsa.edu (J. Moreiras), ep@utulsa.edu, eduardo-pereyra@utulsa.edu (E. Pereyra), cem-sarica@utulsa.edu (C. Sarica), cft@utulsa.edu (C.F. Torres).

¹ Tel.: +1 918 4068387.

² Tel.: +1 918 6315154.

³ Tel.: +1 918 6312152.

1.1. Translational velocity

Translational velocity is defined as the velocity of a slug unit. The expression for translational velocity, v_t , was proposed by Nicklin et al. (1962) as the summation of the total mixture velocity, v_M , multiplied by the flow coefficient, C_o , and the drift velocity, v_d . This is expressed as

$$v_T = C_o v_M + v_d. \quad (1)$$

The flow coefficient, C_o , is an approximate ratio of the maximum to the average velocity of a fully developed velocity profile. For turbulent and laminar flows, C_o is 1.2 and 2.0, respectively (Wallis, 1969). The product of the flow coefficient and the mixture velocity corresponds to the maximum mixture velocity of the slug unit. Based on this expression, the drift velocity is an important parameter of translational velocity, in particular when the mixture velocity is small.

1.2. Drift velocity

Four dimensionless numbers have been identified by previous studies (Wallis, 1969; Weber, 1981; Joseph, 2003) as important terms to characterize drift velocity, namely, Froude, Fr , Eotvos, E_o , Viscosity, N_{vis} , and Reynolds, Re , numbers. Since the viscosity number is obtained by dividing the Froude number by the Reynolds number, only two of them can be used simultaneously.

$$Fr = v_d \rho_L^{0.5} (gD(\rho_L - \rho_G))^{-0.5}. \quad (2)$$

$$E_o = gD^2(\rho_L - \rho_G)\sigma^{-1}. \quad (3)$$

$$N_{vis} = \mu (gD^3(\rho_L - \rho_G)\rho_L)^{-0.5}. \quad (4)$$

$$Re = v_d \rho_L D \mu_L^{-1}. \quad (5)$$

Dumitrescu (1943) and Davies and Taylor (1950) proposed a potential flow solution for the drift velocity determination in vertical flow. Potential flow theory inherently neglects the effects of surface tension and viscosity, yielding a drift velocity model that is only a function of gravitational effects and pipe geometry. The equation proposed was

$$v_d^v = 0.351 \sqrt{gD} \quad (6)$$

Benjamin (1968) followed the potential flow analysis to determine the drift velocity for horizontal flow. He proposed an experimental procedure where the drift velocity for horizontal flow is the same as the velocity of the gas penetration when the liquid is drained out of a horizontal pipe. His experiments provided the following expression for drift velocity.

$$v_d^h = 0.542 \sqrt{gD} \quad (7)$$

Wallis (1969) and Dukler and Hubbard (1975) claimed that drift velocity cannot possibly occur in a horizontal pipe since gravity cannot act in the horizontal direction. However, Nicholson et al. (1978), Weber (1981), and Bendiksen (1984) demonstrated that drift velocity in horizontal flow can be the result of a gravitational potential from the difference in pressure between the top and bottom of the bubble nose. Bendiksen (1984) proposed the correlation of drift velocity for inclined flow as follows:

$$v_d = v_d^h \cos \theta + v_d^v \sin \theta. \quad (8)$$

Zukoski (1966) conducted an experimental program to determine the influence of liquid viscosity, pipe diameter, and surface tension over the drift velocity. The author suggested that, for vertical flow, the drift velocity is independent of surface tension effects if $E_o > 40$. Additionally, for $Re > 100$, the effect of the

viscosity over the bubble rise velocity is negligible. For low Reynolds numbers, $Re < 4$, the drift velocity is inversely proportional to the liquid viscosity. No analysis of the liquid viscosity effect is presented for horizontal or inclined flow. Zukoski (1966) also suggests that as the pipe diameter increases, drift velocity also increases. Finally, the drift velocity describes a convex curve with respect to the inclination angle, reaching a maximum around 45° from the horizontal.

Wallis (1969) suggested that drift velocity in long gas bubbles is governed by Froude, Viscosity, and Eotvos numbers. He mentioned the existence of the dominance of three effects, namely, inertia ($N_{vis} < 0.003$ and $E_o > 100$), viscosity ($N_{vis} > 0.5$ and $E_o > 100$) and surface tension ($E_o = 3.37$). In summary, if the E_o is larger than 100, the effect of surface tension over drift velocity is negligible for vertical flow.

Weber et al. (1986) presented an experimental study to analyze the effect of liquid viscosity on drift velocity for inclined tubes. His data reveals that depending on liquid viscosity, the drift velocity for horizontal flow, v_d^h , can be either smaller or larger than the drift velocity for vertical conditions, v_d^v . In a 0.0373-m ID pipe, $\Delta v_d = v_d^v - v_d^h$ is negative for low viscosities ($\mu_L < 0.0511$ Pa s) and positive for high viscosities ($\mu_L > 0.194$ Pa s). The authors also proposed a correction to Bendiksen (1984) to account for the case of $\Delta v_d < 0$ as follows:

$$v_d = v_d^h \cos \theta + v_d^v \sin \theta + 1.37(\Delta v_d)^{2/3} \sin(\theta)(1 - \sin(\theta)). \quad (9)$$

2. Experimental program

An experimental study to determine drift velocity in medium viscosity oils for different pipe diameters and inclination angles was conducted. This section includes a detailed description of the experimental facility, fluid properties of the test fluids, experimental procedure, instrumentation, the experimental matrix, as well as the uncertainty analysis that was followed for this study.

2.1. Experimental facility

The experimental facility consists of an oil storage tank, a 20 HP screw pump, a 3.05-m (10-ft) long acrylic pipe with 0.0508-m (2-in.) ID, heating and cooling loops, transfer hoses, two transfer tanks, a diaphragm pump, and instrumentation. The heating and cooling loops are used to maintain the desired temperature and thereby control the viscosity of the oil. The acrylic pipe is located close to the storage tank. The inclination of the pipe can be varied from 0° to 90° using a pulley arrangement.

2.2. Properties of test fluids

Compressed air was used as the gas phase and typical properties of the DN-20 mineral oil used in these tests are as follows: (1) gravity: 30.5°API; (2) viscosity: 0.166 Pa s at 21.1°C ; (3) density: 873 kg/m^3 at 15.6°C ; and (4) surface tension: 0.0275 N/m at 40°C .

2.3. Experimental procedure

2.3.1. Inclined pipe

After heating the oil to the required temperature for the desired viscosity, the oil pump is turned on to supply oil to the pipe. Then, the main inlet valve and the auxiliary inlet valve are closed. The drainage valve is opened to drain the residual oil captured and thus to create a gas pocket in the inlet chamber. The pulley arrangement is used to set the pipe at the desired inclination. Next, the drainage valve is closed and the main inlet valve is opened to release the gas bubble into the stagnant oil column.

The drift velocity is measured by recording the bubble penetrating the column with a high speed camera and measuring the time the nose of the bubble travels between two reference points with known distance.

2.3.2. Horizontal pipe

The oil is heated to the required temperature for the desired viscosity. The oil is pumped to the pipe in the vertical position until it is completely filled. A removable plug was designed to close the pipe to ensure the pipe had no air bubbles inside before performing the test. To estimate the drift velocity for the horizontal pipe (0°), the same procedure that is done for inclined flow is performed by draining the inlet chamber of oil and opening the auxiliary inlet valve to allow the gas pocket to penetrate the pipe. A high-speed camera was used to measure the drift velocity.

2.4. Instrumentation

The instrumentation consists of a temperature transducer at the oil tank, a digital angle meter, and a photron high-speed video camera.

2.4.1. Digital angle meter

The inclination angle of the pipe is accurately calculated in degrees by a digital angle meter, $\pm 0.1^\circ$. The pipe is set at the desired angle with a rope and pulley system.

2.4.2. High-speed camera

The system includes a video camera, transfer cable and a processor capable of capturing up to 2000 frames per second (fps) at 1024×1024 pixels resolution. The high-speed videos were


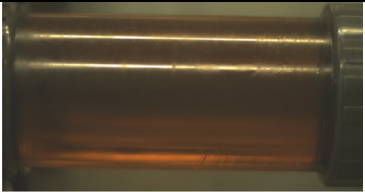
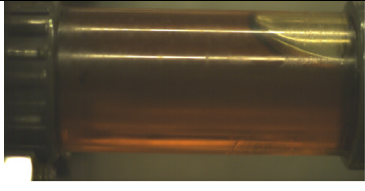
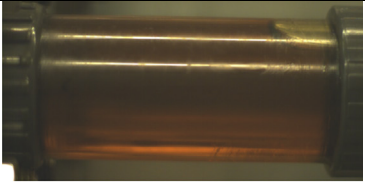
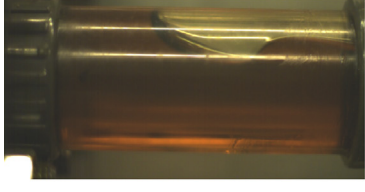
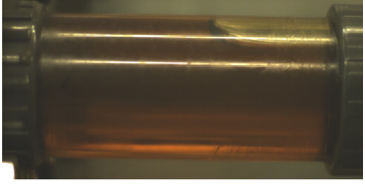
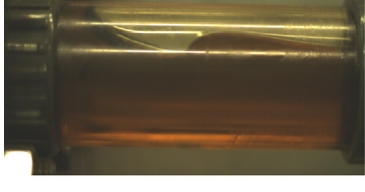
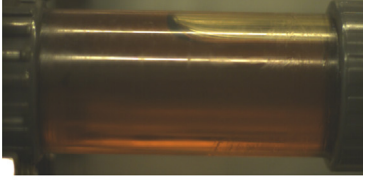
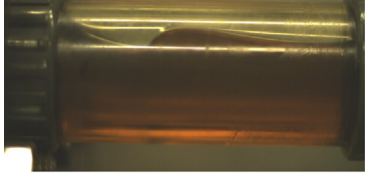
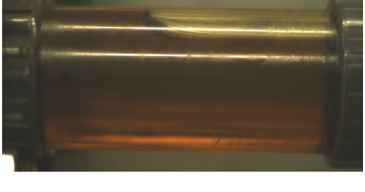
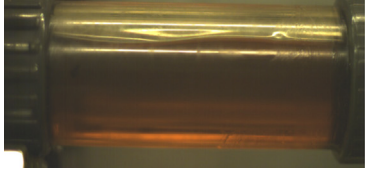
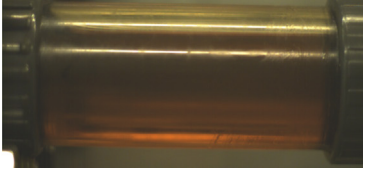
| Time | 0.0508-m Horizontal Flow, 0.039 Pa s | 0.0508-m Horizontal Flow, 0.166 Pa s | Time |
|--------|---|--|--------|
| 0.0s |  |  | 0.0s |
| 0.152s |  |  | 0.152s |
| 0.300s |  |  | 0.300s |
| 0.400s |  |  | 0.400s |
| 0.456s |  |  | 0.456s |
| 0.708s |  |  | 0.708s |

Fig. 1. Comparison of low and high viscosity drift velocity with high speed camera.

typically recorded at 60 fps with normal environment lighting. The resulting video is used to determine the time difference of the bubble traveling in the pipe from the first to the second reference points.

2.5. Experimental matrix

Drift velocity was acquired for the following conditions: (1) pipe diameter: 0.0508 m; (2) inclination angle: 0°, 10°, 20°, ..., 90°; and (3) oil viscosity: 0.039 Pa s, 0.066 Pa s, 0.108 Pa s and 0.166 Pa s.

2.6. Uncertainty analysis

An uncertainty analysis of collected values was performed to account for random errors intrinsic in the collection of empirical data. A variety of reasons can cause random errors and these uncertainties are seldom eliminated. Therefore, quantifying these uncertainties is necessary to understand the level of confidence of the data collected. The uncertainty was estimated using the ASME model for $N=5$ repetitions for each condition and $N-1$ degrees of freedom.

$$U = \pm t \sqrt{b_r^2 + S_{\bar{x}}^2} \quad (10)$$

where U is the random uncertainty, t is the Student t for 95%, b_r is the bias number (neglected under our conditions) and $S_{\bar{x}}$ is the standard deviation of the population average, which is given with the following equation:

$$S_{\bar{x}} = \frac{S_x}{\sqrt{N}} \quad (11)$$

where N is the number of repetitions, and S_x is the sample standard deviation which is given as

$$S_x = \sqrt{\frac{\sum_{i=1}^N (x_i - \bar{x})^2}{N-1}} \quad (12)$$

where x_i is each individual measured data for $i=1-N$ and \bar{x} is the average of the collected data for each individual condition. Each measured data X includes an uncertainty, expressed as $X \pm U$.

3. Experimental results

The experiment was performed for a 0.0508-m ID pipe for horizontal and inclined configurations. The drift velocity was calculated by measuring the time of travel of a fixed point in the bubble body between two fixed points in the pipe.

3.1. Horizontal flow

The results obtained show that the drift velocity increases with decreasing viscosity. As can be seen in Fig. 1 below, the penetrating bubble travels a longer distance in low viscosity oil than in higher viscosity oil in the same amount of time. Thus, the drift velocity is higher for lower viscosity oils than for higher viscosity oils in horizontal flow.

This tendency can also be seen in Figs. 2 and 3, which show the relationship of drift velocity with the fluid temperature, and therefore, with the fluid viscosity.

When the drift velocity is plotted vs. liquid viscosity (Fig. 3) and compared with the data obtained by Gokcal et al. (2008), and the potential flow estimation proposed by Benjamin (1968), it can be observed that the drift velocity follows the trend from Gokcal's experiment but at a lower drift velocity due to differences in fluid density. In addition, it can be observed that both studies have data

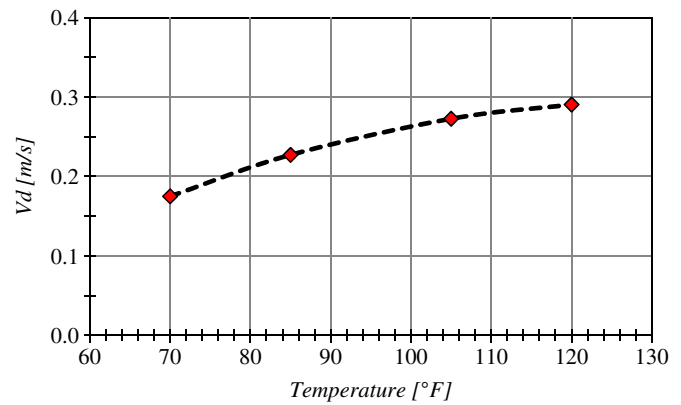


Fig. 2. Drift velocity vs. fluid temperature.

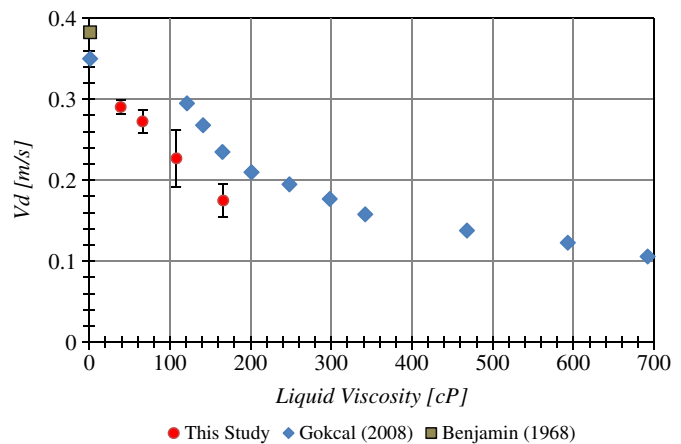


Fig. 3. 2-in. Horizontal flow drift velocity vs. viscosity.

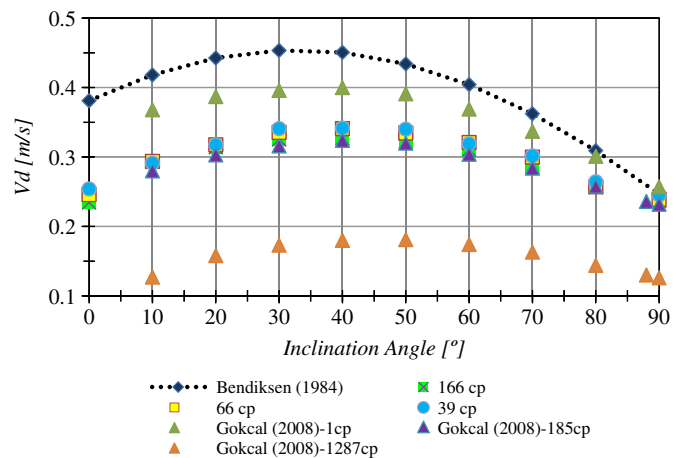


Fig. 4. 2-in. Drift velocity vs. inclination angle.

that approach the potential flow drift velocity as liquid viscosity decreases.

3.2. Inclined flow

The results for inclined flow show that drift velocity increases to a maximum at an inclination angle between 30° and 50° from the horizontal and decreases as the inclination angle approaches 90°. The parabolic trend is also shown by the potential flow solution suggested by Bendiksen (1984). Fig. 4 presents the drift velocity obtained in this study and the drift velocity estimated by

the potential flow solution. This solution overestimates the actual drift velocity measured in a 0.0508-m ID inclined pipe. Additionally, by plotting the data obtained by Gokcal et al. (2008) for high and low viscosities, it is observed that the drift velocity for medium viscosities falls in between the highest and lowest viscosity data, as expected. Hence, it is corroborated that as the viscosity increases, the drift velocity decreases.

It is important to notice as well that, for inclination angles that approach 90°, the difference between drift velocity for the experimental data and the potential flow solution becomes smaller. On the contrary, this difference is significant for angles smaller than 50° and is the largest for the horizontal case.

4. Modeling approach

As mentioned before, the drift velocity in inclined pipes describes a convex parabolic curve as a function of the inclination angle. The shape of this curve is defined by the values of the drift velocity in horizontal and vertical flow. In the next sections, drift velocity correlations for horizontal and vertical flow are proposed and extended to inclined flow. The experimental data collected in this study is combined with literature data. Only pipe diameters larger than 0.03 m have been considered (see Table 1).

4.1. Horizontal flow

In the extended experimental data base presented in Table 1, the Eotvos number varies from 220 to 800. The minimum E_o is at least two times larger than the critical value proposed by Wallis (1969) to define the region where surface tension effects can be neglected ($E_o > 100$). Based on observations by Zukoski (1966), this critical value is even smaller ($E_o > 40$); thus, in this study, the surface tension effect is neglected. Fig. 6 shows the relationship between the Froude and viscosity numbers. As the viscosity number tends to zero, the Froude number tends to the potential flow solution. On the other hand, as the viscosity number increases, the drift velocity tends to zero. Additionally, based on the experimental data given in Fig. 5, the following correlation is proposed for horizontal flow, which is valid for horizontal pipes with diameters larger than 0.03 m.

$$Fr = 0.54 - \frac{N_{vis}}{a + bN_{vis}} \quad (13)$$

where the parameters a and b are given by 1.886 and 0.01443 with confidence intervals of 0.25 and 0.0035, respectively. The general

Table 1
Experimental data base description.

| Author | Fluid properties | Pipe geometry |
|----------------------|---|---|
| Zukoski (1966) | $\rho_L = 1000 \text{ kg/m}^3$ $\mu_L = 0.001 \text{ Pa s}$ $\sigma = 0.072 \text{ N/m}$ | $\theta = 0-90^\circ$ $D = 0.055 \text{ m and } 0.178 \text{ m}$ |
| Weber et al. (1986) | $\rho_L = 1280-1410 \text{ kg/m}^3$ $\mu_L = 0.0511-6.12 \text{ Pa s}$ $\sigma = 0.078-0.087 \text{ N/m}$ | $\theta = 0-90^\circ$ $D = 0.0373 \text{ m}$ |
| Gokcal et al. (2008) | $\rho_L = 889 \text{ kg/m}^3$ $\mu_L = 0.104-0.692 \text{ Pa s}$ $\sigma = 0.029 \text{ N/m}$ | $\theta = 0-90^\circ$ $D = 0.0508 \text{ m}$ |
| Jeyachandra (2011) | $\rho_L = 889 \text{ kg/m}^3$ $\mu_L = 0.154-0.574 \text{ Pa s}$ $\sigma = 0.029 \text{ N/m}$ | $\theta = 0-90^\circ$ $D = 0.0762 \text{ m}$ |
| This study | $\rho_L = 870 \text{ kg/m}^3$ $\mu_L = 0.039-0.166 \text{ Pa s}$ $\sigma = 0.0275 \text{ N/m}$ | $\theta = 0-90^\circ$ $D = 0.0508 \text{ m}$ |

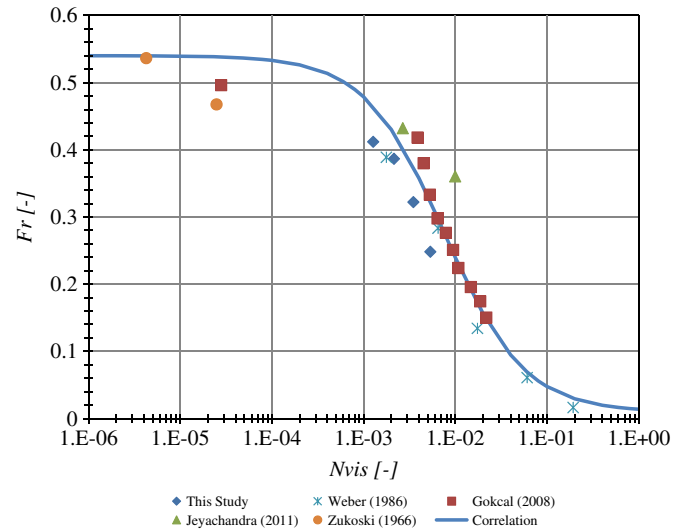


Fig. 5. Froude vs. viscosity number for horizontal flow.

correlation coefficient is given by $r^2 = 0.896$. The proposed correlation is capable of predicting the drift velocity for low and high viscosity ranges for pipe diameters larger than 0.03 m.

4.2. Vertical flow

Joseph (2003) extended Davies and Taylor's (1950) analysis of cap bubbles using viscous potential flow analysis. They proposed a drift velocity expression as a function of viscosity, density, and pipe diameter as follows:

$$v_d = -\frac{8}{3} \frac{\mu_L}{\rho_L D} + \sqrt{\frac{2}{9} g D + \frac{64}{9} \frac{\mu_L^2}{(\rho_L D)^2}} \quad (14)$$

For long bubbles (Taylor bubble type), Joseph (2003) showed a systematic bias with respect to the experimental data in vertical flow (see Fig. 7a). As the viscosity tends to zero ($\mu_L \rightarrow 0$), Eq. (14) tends to $v_d = k \sqrt{g D}$ (potential flow), where the shape factor, k , is given by $\sqrt{2}/3$. This result is in agreement with Davies and Taylor's (1950) solution for cap bubbles. Davies and Taylor (1950) also proposed an extension of the cap model to long bubbles. The extension resulted in a modification of the shape factor to $k = 0.328$. This result differs slightly from the solution proposed by Dumitrescu (1943) where $k = 0.351$. As referred by Viana et al. (2003), the most accepted value for shape factor is $k = 0.35$. This difference in the potential flow solution between the cap-shaped bubble and long bubble can explain the bias presented in Fig. 6a. The discrepancy can be corrected in a similar way as Davies and Taylor (1950) proposed, by subtracting the difference of potential solutions from Eq. (14) as follows:

$$v_d = -\frac{8}{3} \frac{\mu_L}{\rho_L D} + \sqrt{\frac{2}{9} g D + \frac{64}{9} \frac{\mu_L^2}{(\rho_L D)^2}} - \left(\frac{\sqrt{2}}{3} - 0.35 \right) \sqrt{g D} \quad (15)$$

As illustrated in Fig. 6b, Eq. (15) presents better agreement with experimental data as compared with Eq. (14). Eq. (15) is suitable for low and high viscosity ranges.

4.3. Inclined flow

The Froude number in any inclination can be predicted by a combined effect of horizontal and vertical Froude number as follows:

$$Fr = Fr_H \cos(\theta)^a + Fr_V \sin(\theta)^b + Q \quad (16)$$

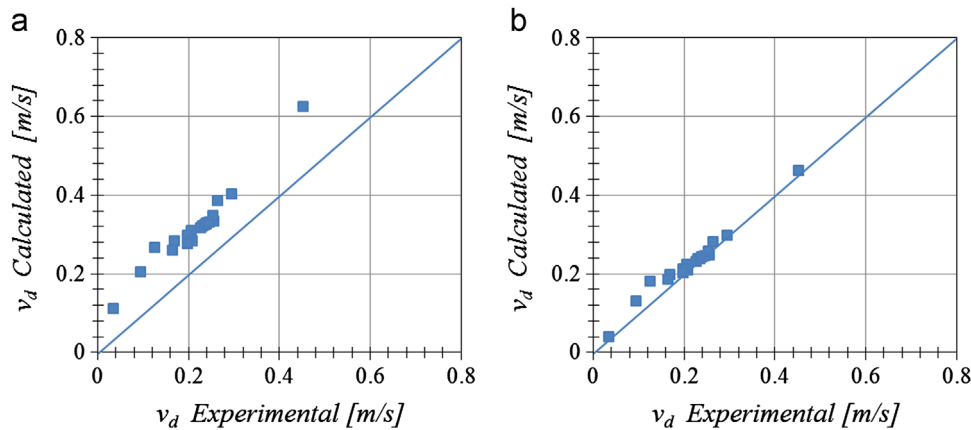


Fig. 6. Calculated drift velocity by Joseph (2003) vs. experimental for vertical flow. (a) Original and (b) corrected for potential flow solution.

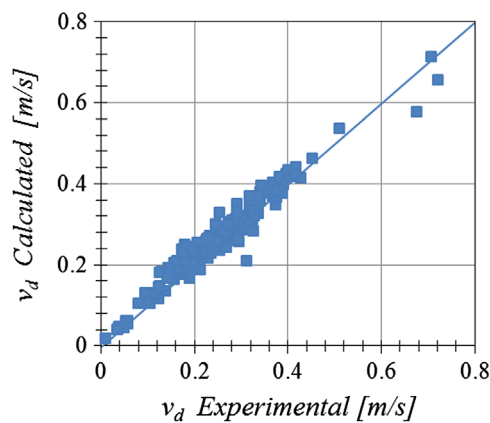


Fig. 7. Calculated drift velocity vs. experimental drift velocity.

This correlation is similar to Weber's (1981) correlation, where Q is given as follows:

$$\begin{aligned} \text{If } (Fr_V - Fr_H) < 0; \quad Q &= 0 \\ \text{If } (Fr_V - Fr_H) \geq 0; \quad Q &= c(Fr_V - Fr_H)^d \sin(\theta)(1 - \sin(\theta)) \end{aligned} \quad (17)$$

Using all the available data points presented in Table 1 for inclined flow, the final correlation coefficient for Eq. (16) is given by $r^2=0.94$. Experimental Froude number for vertical and horizontal cases has been considered. Table 2 provides the final values for each corresponding parameter and their 95% confidence interval. As demonstrated by the 95% confidence interval, the parameters (a , b , c , and d) cannot be zero or one, indicating that these terms are significant in describing the phenomenon.

4.4. Calculation procedure

The generalized Froude number for any inclination angle is calculated as follows:

1. Calculate the viscosity number using Eq. (4).

$$N_{vis} = \mu \left(gD^3(\rho_L - \rho_G) \right)^{-0.5} \quad (4)$$

2. Calculate the horizontal Froude number using Eq. (13).

$$Fr_H = 0.54 - \frac{N_{vis}}{1.886 + 0.01443N_{vis}} \quad (13)$$

Table 2
Fitted parameters for inclined flow correlation.

| Parameter | Value | 95% Confidence interval |
|-----------|---------|-------------------------|
| a | 1.2391 | 0.0872 |
| b | 1.2315 | 0.1150 |
| c | 2.1589 | 1.4764 |
| d | 0.70412 | 0.2926 |

3. Calculate the vertical Froude number using the dimensionless form of Eq. (15).

$$Fr_V = -\frac{8}{3}N_{vis} + \sqrt{\frac{2}{9}\frac{\rho_L}{\rho_L - \rho_G} + \frac{64}{9}N_{vis}^2} - \left(\frac{\sqrt{2}}{3} - 0.35\right) \sqrt{\frac{\rho_L}{\rho_L - \rho_G}} \quad (18)$$

4. Calculate Q .

$$\text{If } (Fr_V - Fr_H) < 0; Q = 0$$

$$\text{If } (Fr_V - Fr_H) \geq 0; Q = c(Fr_V - Fr_H)^d \sin(\theta)(1 - \sin(\theta)) \quad (17)$$

5. Calculate the generalized Froude number using Eq. (16).

$$Fr = Fr_H \cos(\theta)^a + Fr_V \sin(\theta)^b + Q \quad (16)$$

6. The drift velocity is finally calculated solving Eq. (2).

$$v_d = Fr \rho_L^{-0.5} (gD(\rho_L - \rho_G))^{0.5} \quad (19)$$

The overall average absolute value of the relative error of the correlation is 12.9%. The model is verified against all the data available in Fig. 7, showing good agreement for all the different viscosity and pipe diameter ranges considered. The uncertainty of the fitted parameters can be propagated to the calculated drift velocity using series Taylor expansion, assuming that the parameters are mutually independent and normally distributed. This procedure was shown by Pereyra et al. (2012).

4.5. Summary and discussion

The horizontal and vertical Froude numbers asymptotically achieve their theoretical values when the viscosity number tends to zero. In contrast, as the viscosity numbers tend to one, the horizontal Froude decreases almost to zero, but for vertical case there is a maximum value of the viscosity number close to

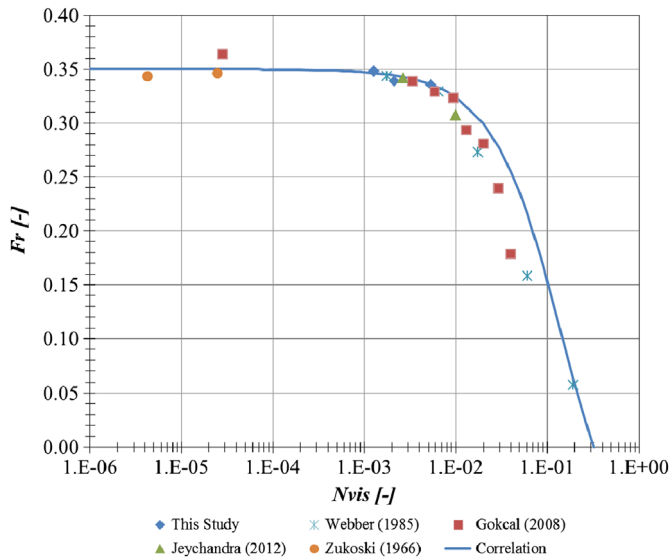


Fig. 8. Calculated drift velocity vs. experimental drift velocity.

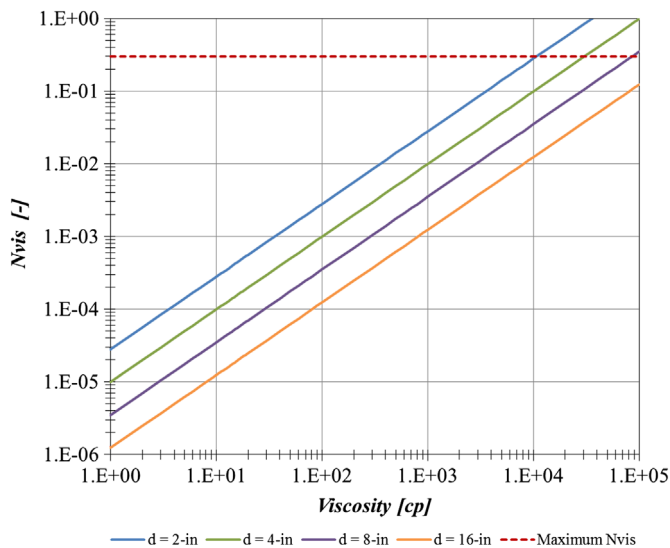


Fig. 9. Viscosity number for different pipes diameters.

0.3 depending slightly on the gas density. Fig. 8 shows the behavior of the vertical Froude number neglecting the effect of the gas density.

Fig. 9 illustrates that the viscosity number linear increases with the viscosity, and it is inversely proportion to the pipe diameter. The effect of the gas density on viscosity number is small and was neglected to construct the figure.

As can be seen from Fig. 9, as the pipe diameter increases, the maximum viscosity that can be used in the correlation increases. For large pipe diameters, Taylor bubbles have been observed in vertical pipes (Zabaras et al., 2013), and recently Pringle et al. (in press) reported stable Taylor bubbles in large pipes diameters. The proposed correlation is valid for any combination of variables in the viscosity number if they fall within the range given in Table 3, and if the bubbles 4–5 times larger than the pipe.

5. Concluding remarks

The effect of medium oil viscosities, ranging from 0.039 Pa s to 0.166 Pa s, as well as the impact of the inclination angle from

Table 3
Viscosity numbers ranges.

| Parameter | N_{vis} range |
|-----------|-----------------|
| Fr_H | 0–1 |
| Fr_V | 0–0.3 |
| Q | 0–0.3 |

0° to 90°, and the pipe diameter on drift velocity was investigated. It was observed from the experiments that drift velocity decreases as the viscosity of the oil increases. Furthermore, experimental results demonstrated that liquid viscosity has a larger impact on the drift velocity for each inclination than the inclination has for each viscosity. Both, however, have important effects on drift velocity. Comparing the drift velocity range for each pipe diameter, a larger pipe will cause the drift velocity to be higher.

Based on the data acquired in this study and the data collected from the literature, a unified correlation to estimate drift velocity in low and high viscosity oils in dimensionless form was developed. This correlation can predict the drift velocity for a broad range of viscosities, pipe diameters, and inclination angles. Performing experiments that consider the range between a viscosity number of 10^{-4} and 10^{-3} is strongly suggested to obtain experimental values in the transition region from viscosity affected to potential flow solution in horizontal flow.

Acknowledgments

Tulsa University Fluid Flow Project (TUFP) members are acknowledged for their support of this project. Ms. Rosmer Brito, a Ph.D. student at the University of Tulsa is acknowledged for her contributions in experimental part of the study. Mr. Eleazar Palomo is thanked for volunteering his time to this research.

References

- Benjamin, T.B., 1968. Gravity currents and related phenomena. *J. Fluid Mech.* 31 (Part 2), 209–248.
- Bendiksen, K.H., 1984. An experimental investigation of the motion of long bubbles in inclined tubes. *Int. J. Multiph. Flow* 10, 467–483.
- Brito, R., 2012. Effect of Medium Oil Viscosity on Two-Phase Oil–Gas Flow Behavior in Horizontal Pipes (M.S. thesis). The University of Tulsa, Tulsa, OK.
- Davies, R.M., Taylor, G.I., 1950. The mechanics of large bubbles rising through liquids in tubes. *Proc. R. Soc. Lond. Ser. A* 200, 375–390.
- Dukler, A.E., Hubbard, M.G., 1975. A model for gas–liquid slug flow in horizontal and near-horizontal tubes. *Ind. Eng. Chem. Fund.* 14 (347), 337.
- Dumitrescu, D.T., 1943. Strömung an einer Luftblase im senkrechten Rohr. *Z. Angew. Mat. Mech.* 23, 139–149.
- Gokcal, B., 2005. (M.S. thesis). Effects of High Oil Viscosity on Two-Phase Oil–Gas Flow Behavior in Horizontal Pipes. The University of Tulsa, Tulsa, OK.
- Gokcal, B., Al-Sarkhi, A., Sarica, C., 2008. Effects of High Oil Viscosity on Drift Velocity for Horizontal Pipes. Presented at BHR Conference of Multiphase Production Technology. Banff, Canada, June 4–6.
- Jeyachandra, B., 2011. (M.S. thesis). Effect of Pipe Inclination on Flow Characteristics of High Viscosity Oil–Gas Two-Phase Flow. The University of Tulsa, Tulsa, OK.
- Joseph, D.D., 2003. Rise velocity of a spherical cap bubble. *J. Fluid Mech.* 488, 213–223.
- Kora, Y., 2010. (M.S. thesis). Effects of High Oil Viscosity on Slug Liquid Holdup in Horizontal Pipes. The University of Tulsa, Tulsa, OK.
- Nicklin, D.J., Wilkes, J.O., Davidson, J.F., 1962. Two-phase flow in vertical tubes. *Trans. Inst. Chem. Eng.* 40, 61–68.
- Nicholson, M.K., Aziz, K., Gregory, G.A., 1978. Intermittent two-phase flow in horizontal pipes: predictive models. *Can. J. Chem. Eng.* 56, 389–399.
- Pereyra, E., Arismendi, R., Gomez, L.E., Mohan, R.S., Shoham, O., Kouba, G.E., 2012. State of the art of experimental studies and predictive methods for slug liquid holdup. *J. Energy Resour. Technol.* 134, 023001.
- Pringle, C.T.C., Ambroseb, S., Azzopardib, B.J., Rustc, A.C. The existence and behaviour of large diameter Taylor bubbles. *Int. J. Multiph. Flow* (in press).
- Viana, F., Pardo, R., Yanez, R., Trallero, J.L., Joseph, D.D., 2003. Universal correlation for the rise velocity of long gas bubbles in round pipes. *J. Fluid Mech.* 494, 379–398.

Wallis, G.B., 1969. One Dimensional Two-Phase Flow. McGraw-Hill, New York.

Weber, M.E., 1981. Drift in intermittent two-phase flow in horizontal pipes. *Can. J. Chem. Eng.* 59, 398–399.

Weber, M.E., Alarie, A., Ryan, M.E., 1986. Velocities of extended bubbles in inclined tubes. *Chem. Eng. Sci.* 41, 2235–2240.

Zabaras, G., Menon, R., Schoppa, W., Wicks, M., 2013. Presented at Offshore Technology Conference. Houston, Texas, May 6–9.

Zukoski, E.E., 1966. Influence of viscosity, surface tension, and inclination angle on motion of long bubbles in closed tubes. *J. Fluid Mech.* 25, 821–837.